

1 **Increased S6K1 phosphorylation protects against early steps of Tau aggregation under**  
2 **long-term mitochondrial stress**

3

4 **Lukasz Samluk\*, Piotr Ostapczuk and Magdalena Dziembowska**

5

6 Centre of New Technologies, University of Warsaw, S. Banacha 2c, 02-097 Warsaw, Poland.

7

8 **\*Correspondence:** [l.samluk@cent.uw.edu.pl](mailto:l.samluk@cent.uw.edu.pl)

9

10

11

12

13

14

15

16

17

18

19

20

21

22

23

24

25

26 **Abstract**

27 Many studies demonstrated the influence of mitochondrial stress on cytosolic signaling  
28 pathways. Here, we found that in cells upon long-term mitochondrial stress, phosphorylation  
29 of S6K1 protein, which is the mTOR pathway component, was increased, like in brains of  
30 Alzheimer's disease (AD) patients. We checked if increased S6K1 phosphorylation was  
31 involved in Tau protein aggregation, which is one of AD hallmarks. HEK239T NDUFA11-  
32 deficient cells treatment with the mTOR inhibitor, INK128, or with S6K1 inhibitor,  
33 PF-4708671, caused the elevation of Tau aggregation. In contrast, stable overactivation of the  
34 mTOR pathway caused a further increase of S6K1 phosphorylation and reduced Tau  
35 oligomerization in HEK239T NDUFA11-deficient cells. Thus, we conclude that the increase  
36 in S6K1 phosphorylation is protective against Tau aggregation under mitochondrial stress.

37

38 **Keywords:** mitochondrial stress; mTOR pathway; S6K1 protein; protein aggregation; Tau  
39 protein; neurodegeneration

40

41

42

43

44

45

46

47

48

49

50

## 51 **Abbreviations**

52 AD, Alzheimer's disease; AMPK, adenosine monophosphate-activated protein kinase; BiFC,  
53 bimolecular fluorescence complementation; DEPTOR, DEP domain-containing mTOR-  
54 interacting protein; DMEM, Dulbecco's Modified Eagle Medium; DTT, dithiothreitol; EDTA,  
55 ethylenediaminetetraacetic acid; GAPDH, glyceraldehyde-3-phosphate dehydrogenase;  
56 mLST8, mammalian lethal with SEC thirteen 8; mTOR, mechanistic target of rapamycin;  
57 mTORC1, mTOR complex 1; NDUFA11, NADH:ubiquinone oxidoreductase subunit A11;  
58 PBS, phosphate-buffered saline; PMSF, phenylmethylsulfonyl fluoride; PRAS40, proline-rich  
59 AKT substrate of 40 kDa; Raptor, regulatory-associated protein of mTOR; S6K1, ribosomal  
60 protein S6 kinase 1; SDS-PAGE, sodium dodecyl sulfate-polyacrylamide gel electrophoresis;  
61 SEM, standard error of the mean; TSC2, tuberous sclerosis complex 2

62

## 63 **Introduction**

64 Mitochondrial dysfunctions are considered as one of the causes of neurodegenerative  
65 diseases. Their potential involvement in the development of neurodegeneration is not only  
66 narrowed to the influence on energy metabolism. Accumulating data demonstrate that  
67 mitochondrial stress affects signaling pathways crucial for protein homeostasis and neuronal  
68 functions (Cabral-Costa and Kowaltowski, 2020). An example is the mTOR pathway which  
69 one of the numerous functions is the regulation of cellular protein synthesis via the mTORC1  
70 complex (Fig. 1A). In our previous studies (Topf *et al.*, 2018; Samluk *et al.*, 2019) we have  
71 shown that dysfunctional mitochondria influence cellular protein homeostasis via the regulation  
72 of protein synthesis. Mitochondrial stress, accompanied by oxidative stress directly affected  
73 ribosomes by the oxidation of cysteine residues in ribosomal proteins (Topf *et al.*, 2018) or by  
74 decreased phosphorylation of mTOR substrate, S6K1 protein, which resulted in  
75 dephosphorylation of S6 ribosomal protein (Samluk *et al.*, 2019). It was demonstrated that the

76 inhibition of cytosolic protein synthesis reduced mitochondrial degeneration (Wang *et al.*,  
77 2008) but prolonged induction of mechanisms that reduce translation under mitochondrial stress  
78 caused a loss of dendrites in neurons of *Drosophila melanogaster* (Tsuyama *et al.*, 2017). Thus,  
79 to avoid cellular death, under long-term mitochondrial stress, protein synthesis needs to be  
80 restored. One of the mechanisms, which ensures a sufficient level of protein synthesis for cell  
81 survival under long-term mitochondrial stress is increased phosphorylation of S6K1 protein  
82 (Samluk *et al.*, 2019). Interestingly, elevated S6K1 phosphorylation is also characteristic of the  
83 brains of Alzheimer's disease patients, in which  $\beta$ -amyloid and Tau protein aggregates can be  
84 observed (An *et al.*, 2003).

85         A few recent studies demonstrated a direct impact of mitochondrial dysfunctions on the  
86 aggregation of proteins that are involved in the development of neurodegenerative diseases.  
87 The accumulation of mitochondrial precursor proteins in the cytosol as a result of mitochondrial  
88 protein import defects, induced the aggregation of  $\alpha$ -synuclein and amyloid  $\beta$  (Nowicka *et al.*,  
89 2021a). Importantly, cytosolic protein aggregates were more efficiently cleared upon the  
90 stimulation of mitochondrial protein import (Nowicka *et al.*, 2021b; Schlagowski *et al.*, 2021).  
91 Moreover, it was shown that long-term mitochondrial stress induced early steps of Tau  
92 aggregation by increasing reactive oxygen species levels and affecting cellular proteostasis  
93 (Samluk *et al.*, 2022). Interestingly, the increase in mitochondrial proteostasis by targeting  
94 mitochondrial translation and mitophagy reduced amyloid  $\beta$  aggregation in cells, worms and in  
95 transgenic mouse models of Alzheimer's disease (Sorrentino *et al.*, 2017). A previous study  
96 revealed that in mitochondrial prohibitin PHB2-deficient hippocampal neurons, Tau protein  
97 was hyperphosphorylated and aggregated but the mechanism of this phenomenon is still not  
98 known (Merkwirth *et al.*, 2012).

99 In this study, we confirmed increased phosphorylation of S6K1 protein and enhanced Tau  
100 aggregation in mammalian cells under long-term mitochondrial stress. In order to monitor early

101 steps of Tau aggregation, we performed the bimolecular fluorescence complementation (BiFC)  
102 assay using HEK293T cells that were treated with rotenone or HEK293T cells with  
103 TALEN-mediated knockout of gene encoding mitochondrial protein, NDUFA11 (Stroud *et al.*,  
104 2016). We demonstrated that mTOR and S6K1 inhibition with INK128 and PF-4708671,  
105 respectively, led to the escalation of Tau oligomerization in HEK293T NDUFA11-deficient  
106 cells. On the contrary, shRNA-mediated knockdown of TSC2 protein in HEK293T NDUFA11  
107 knockout cells, which induced overactivation of the mTOR pathway and further increased  
108 S6K1 phosphorylation, caused the reduction of early steps of Tau aggregation. In the light of  
109 these findings, we consider increased phosphorylation of S6K1 as a beneficial adaptive  
110 response under long-term mitochondrial stress.

111

## 112 **Materials and methods**

### 113 **Cell culture conditions**

114 HEK293T cells were cultured in high-glucose (4.5 g/L) 90% Dulbecco's Modified  
115 Eagle Medium (DMEM; Sigma, catalog no. D5671) supplemented with 10% FBS, 2 mM  
116 L-glutamine, 100 U/ml penicillin, 0.1 mg/ml streptomycin, and 50 µg/ml uridine at 37°C in a  
117 5% CO<sub>2</sub> humidified atmosphere. The cells were treated with rotenone (48 or 72 h) (Sigma,  
118 catalog no. R8875), mTOR kinase inhibitor (INK128, 3 h) (APExBIO, catalog no. MLN0128),  
119 and S6K1 inhibitor (PF-4708671, 24 h) (Sigma, catalog no. 559273) where indicated.  
120 HEK293T wild type and HEK293T NDUFA11 knockout cells were provided by David Stroud  
121 and Michael Ryan (Monash University, Melbourne, Australia) (Stroud *et al.*, 2016). HEK293T  
122 NDUFA11 knockout cell line with shRNA-mediated knockdown of TSC2 was provided by  
123 Malgorzata Urbańska and Jacek Jaworski (International Institute of Molecular and Cell  
124 Biology, Poland) (Samluk *et al.*, 2019).

125

## 126 **Cell culture transfection**

127 HEK293T cells were seeded in 60 mm cell culture dishes and grown to reach 20-25%  
128 confluence on the day of transfection. For transfection of one plate, 6  $\mu$ l of GeneJuice  
129 Transfection Reagent (Sigma, catalog no. 70967) was mixed thoroughly with 250  $\mu$ l of Opti-  
130 MEM I Reduced Serum Medium (Gibco, catalog no. 31-985-070) and incubated for 5 min at  
131 room temperature. Next, purified plasmid DNA was added at a concentration of 0.5 or 1  
132  $\mu$ g/plate according to the specific experiment, gently mixed by pipetting and incubated for 15  
133 min at room temperature. Then, GeneJuice/DNA mixture was added dropwise to each plate that  
134 contained 5 ml of complete high-glucose DMEM and gently rocked.

135

## 136 **Bimolecular fluorescence complementation**

137 Bimolecular fluorescence complementation (BiFC) assay was performed to monitor the  
138 oligomerization of Tau protein (Fig. 2A) (Tak *et al.*, 2013; Lim *et al.*, 2014). HEK293T cells  
139 were transfected for 72 h with plasmids that encoded Tau protein that was fused to the N-  
140 terminal part of Venus protein, Tau-VN (VN-Tau (wt), Addgene, catalog no. 87368) and Tau  
141 protein that was fused to the C-terminal part of Venus protein, Tau-VC (Tau (wt) -VC,  
142 Addgene, catalog no. 873690) (Blum *et al.*, 2015). The fluorescence of reconstituted Venus  
143 protein, which reflects Tau dimerization, was analyzed using a flow cytometer (BD  
144 LSRFortessa), a fluorescence microplate reader (Ex/Em 488/528) (Synergy H1 Hybrid Multi-  
145 Mode Microplate Reader, BioTek) and Zeiss LSM700 confocal microscope. Fluorescence was  
146 normalized to transfection efficiency that was verified by immunoblotting where indicated.

147

## 148 **Immunofluorescence**

149 HEK293T cells were transfected with BiFC plasmids for 72 h. The cells were then  
150 washed twice with PBS, fixed with 3.7% formaldehyde for 10 min at 4°C, washed again with

151 PBS, and permeabilized for 5 min by treatment with 0.1% Triton X-100 in PBS. Then, cells  
152 were rinsed once with PBS and once with water. The samples were mounted in ProLong  
153 Diamond Antifade Mountant with DAPI (Thermo Fisher Scientific, catalog no. P36962) and  
154 analyzed with a confocal microscope (Zeiss LSM700).

155

## 156 **Miscellaneous**

157 The RIPA buffer was used for the preparation of protein extracts. It contained 65 mM Tris-HCl  
158 (pH 7.4), 150 mM NaCl, 1% IGEPAL CA-630 (NP-40), 0.25% sodium deoxycholate, 1 mM  
159 EDTA, 2 mM PMSF (Sigma, catalog no. P7626), and phosphatase inhibitor cocktail  
160 (PhosSTOP, Roche, catalog no. 04 906 837 001). Proteins in Laemmli sample buffer that  
161 contained 50 mM dithiothreitol (DTT) were denatured at 65°C for 15 min. Total protein extracts  
162 were separated by SDS-PAGE on 12% gels. The following commercially available antibodies  
163 were used: S6K1 (Cell Signaling Technology, catalog no. 9202), Phospho-S6K1 (Thr389) (Cell  
164 Signaling Technology, catalog no. 9205), Phospho-S6 (Ser235/236) (Cell Signaling  
165 Technology, catalog no. 2211), S6 (Cell Signaling Technology, catalog no. 2217), Tau (TAU-  
166 5) (Merck, catalog no. 577801), GAPDH (Santa Cruz Biotechnology, catalog no. sc-47724),  
167 and TSC2 (Cell Signaling Technology, catalog no. 3612). Protein bands were visualized using  
168 secondary antibodies conjugated with horseradish peroxidase and chemiluminescence.  
169 Chemiluminescence signals were detected using Amersham Imager 600 RGB or x-ray films.  
170 Adobe Photoshop CS4 software was used for the digital processing of images and ImageJ  
171 software was used to quantify the immunoblots. The represented fold changes are means of fold  
172 changes that were obtained from independent biological replicates  $\pm$  SEM. VN-Tau (wt) was a  
173 gift from Tiago Outeiro (Addgene plasmid no. 87368; <http://n2t.net/addgene:87368>;  
174 RRID:Addgene\_87368; (Blum *et al.*, 2015). Tau (wt)-VC was a gift from Tiago Outeiro  
175 (Addgene plasmid no. 87369; <http://n2t.net/addgene:87369>; RRID:Addgene\_87369; (Blum *et*

176 *al.*, 2015). pRK5-EGFP-Tau AP was a gift from Karen Ashe (Addgene plasmid no. 46905;  
177 <http://n2t.net/addgene:46905>; RRID:Addgene\_46905; (Hoover *et al.*, 2010).

178

## 179 **Statistical analysis**

180 Statistical Student's t test or one-way ANOVA were performed using GraphPad Prism.  
181 Student's t test or one-way ANOVA results are indicated consistently in all figures as \* $p < 0.05$ ,  
182 \*\* $p < 0.01$ , \*\*\* $p < 0.001$  and ns for not significant ( $p > 0.05$ ).

183

## 184 **Results**

### 185 **Long-term mitochondrial stress increase S6K1 phosphorylation**

186 In our previous study we found that upon long-term mitochondrial dysfunctions  
187 phosphorylation of S6K1 was increased, contrary to short-term mitochondrial stress (Samluk  
188 *et al.*, 2019). Interestingly, increased S6K1 protein phosphorylation was also observed in  
189 neurons treated for 6 h with mitochondrial stressors such as oligomycin and  
190 rotenone/antimycin-A, but this phenomenon was not explained (Zheng *et al.*, 2016). Here, we  
191 confirm our previous observations that long-term mitochondrial stress is leading to the increase  
192 in the phosphorylation of S6K1 protein. HEK293T cells that were treated for 48 h with rotenone  
193 and HEK293T NDUFA11-deficient cells (impaired complex I-mediated respiration), exhibited  
194 enhanced phosphorylation of Thr389 residue of S6K1, as demonstrated by immunoblotting  
195 with the use of the antibody that recognizes this specific phospho-residue (Thr389) (Fig. 1B  
196 and C). In HEK293T NDUFA11 knockout cells the increase of S6K1 phosphorylation was  
197 observed despite the moderate reduction of the expression of this protein (Fig. 1B). In contrast,  
198 in HEK293T wild type cells expression of S6K1 protein was growing with the increase of  
199 applied rotenone concentration but anyway the increase of phosphorylation was much stronger  
200 than the increase of the S6K1 expression (Fig 1C). The highest S6K1 phosphorylation was



201 observed in HEK293T wild type cells that received the highest dose of rotenone (100 nM) (Fig  
202 1C), suggesting that the observed phenomenon is dependent on the intensity of mitochondrial  
203 stress. These results demonstrate that long-term mitochondrial stress lead to the increase of  
204 S6K1 phosphorylation.

205

206 **Reduction of the phosphorylation and activity of S6K1 under long-term mitochondrial**  
207 **stress leads to the increase of Tau aggregation**

208 Previously, we have shown that enhanced phosphorylation of S6K1 caused increased  
209 phosphorylation of S6 ribosomal protein to stimulate ribosomes for protein synthesis under  
210 mitochondrial stress (Samluk *et al.*, 2019). This adaptive response probably enabled sufficient  
211 protein synthesis and cell survival under these conditions but its effect on cellular proteostasis  
212 was unknown. Since the elevation of S6K1 activity was also observed in the brains of  
213 Alzheimer's disease (AD) patients (An *et al.*, 2003), we decided to check the influence of the  
214 increase of S6K1 phosphorylation on Tau protein aggregation. In order to monitor the early  
215 steps of Tau aggregation, we performed the bimolecular fluorescence complementation (BiFC)  
216 assay, which principle is shown in figure 2A. Tau protein dimerization and oligomerization  
217 were reflected by the increase in the fluorescence of Venus protein, which was detected using  
218 flow cytometry (Fig. 2B and D) and confocal microscopy (Fig. 2C). We confirmed our previous  
219 observations (Samluk *et al.*, 2022) that Tau protein aggregation increased in HEK293T  
220 NDUFA11-deficient cells and HEK293T cells that were treated for 72 h with rotenone in a  
221 concentration-dependent manner (Fig. 2B, 2C and 2D). To determine the effect of the S6K1  
222 phosphorylation on Tau aggregation we performed the BiFC assay in HEK293T NDUFA11  
223 knockout cells that were treated for 3 h with INK128 (30 and 75 nM), which is an inhibitor of  
224 mTOR kinase (Fig. 3A). The phosphorylation of S6K1 was significantly reduced despite the  
225 increase in S6K1 expression upon cells treatment with INK128. Inhibition of mTOR activity

226 under long-term mitochondrial stress resulted in the increase in the fluorescence that reflected  
227 Tau aggregation and it was dependent on increasing INK128 concentration (Fig. 3A). The  
228 results of fluorescence measurements were normalized to levels of Tau expression detected by  
229 immunoblotting to avoid the potential influence of unequal cell transfection. Next, in order to  
230 investigate the specific effect of S6K1 activity on Tau aggregation, BiFC assay was performed  
231 using HEK293T NDUFA11-deficient cells that were treated for 24 h with S6K1 inhibitor (20  
232 and 50  $\mu$ M), PF 4708671 (Fig. 3B). We observed dephosphorylation of S6 protein  
233 (Ser235/236), which is an S6K1 substrate, indicating that the activity of S6K1 was blocked.  
234 The normalized fluorescence was increased upon cells treatment with PF-4708671, showing  
235 that reduction of S6K1 activity led to the increase in Tau dimerization (Fig. 3B). These results  
236 demonstrated that inhibition of S6K1 phosphorylation and activity in NDUFA11 KO HEK293T  
237 cells triggered an increase in early steps of Tau aggregation.

238

239 **The activation of the mTOR pathway and the increase in the phosphorylation of S6K1**  
240 **leads to the reduction of Tau aggregation under long-term mitochondrial stress**

241 Next, we investigated whether activation of the mTOR pathway under conditions of  
242 long-term mitochondrial stress reduces Tau dimerization. Stable overactivation of the mTOR  
243 pathway was achieved by shRNA-mediated knockdown of TSC2 protein, which is a part of a  
244 protein complex that inhibits the mTOR pathway (Fig. 1A). As shown in figure 4A the level of  
245 TSC2 expression detected by immunoblotting was reduced approximately two times by specific  
246 shRNA compared to the control HEK293T NDUFA11-deficient cells. The knockdown of TSC2  
247 led to the further increase of S6K1 phosphorylation at Thr389 and S6 protein at Ser235/236,  
248 suggesting overactivation of mTOR pathway (Fig. 4B). Next, we performed the BiFC assay.  
249 The fluorescence, normalized to Tau expression levels, was significantly decreased in  
250 HEK293T NDUFA11-deficient cells with a knockdown of TSC2 protein (Fig. 4B), indicating

251 lower Tau dimerization under these conditions. Our results show that the activation mTOR  
252 pathway and increased S6K1 phosphorylation cause a significant reduction of early steps of  
253 Tau aggregation under long-term mitochondrial stress.

254

## 255 **Discussion**

256 Mitochondria, besides their primary function in energy production, are nowadays perceived as  
257 important signaling organelles. Under stress conditions, they affect signaling pathways that  
258 maintain protein homeostasis (proteostasis) in the cell. This fact puts mitochondria in a center  
259 of interest in studies investigating causes of neurodegenerative diseases, in which proteostasis  
260 defects and protein aggregation are observed. In the present and our previous study, we  
261 observed that long-term mitochondrial stress induce early steps of Tau aggregation (Samluk *et*  
262 *al.*, 2022), characteristic of tauopathies, such as Alzheimer's disease (AD). Previously we also  
263 demonstrated that mitochondrial dysfunctions affected the mTOR pathway (Samluk *et al.*,  
264 2019). This pathway among others regulates protein synthesis in the cell via phosphorylation  
265 of S6K1 protein that phosphorylates S6 ribosomal protein. Under the short-term mitochondrial  
266 stress phosphorylation of S6K1 was reduced, in contrast to long-term mitochondrial stress  
267 under which S6K1 phosphorylation was enhanced. Our interpretation of this phenomenon was  
268 that short-term inhibition of protein synthesis was beneficial for restoring protein homeostasis,  
269 while long-lasting protein synthesis inhibition may lead to the insufficient synthesis of crucial  
270 proteins and cellular death (Samluk *et al.*, 2019). Thus, increased phosphorylation of S6K1  
271 under long-term mitochondrial stress may be a pro-survival response but its effect on general  
272 protein homeostasis remains unknown. Two studies linked mitochondrial stress, increased  
273 S6K1 phosphorylation and neurodegeneration. The increase in S6K1 protein phosphorylation  
274 was observed in neurons that were treated for 6 h with compounds that affect mitochondrial  
275 function, oligomycin and rotenone/antimycin-A, (Zheng *et al.*, 2016). Interestingly, the

276 elevation of S6K1 activity was also observed in the brains of Alzheimer's disease patients (An  
277 *et al.*, 2003). In the present study, we studied the influence of the mTOR pathway activity and  
278 increased S6K1 phosphorylation on early steps of Tau aggregation. We demonstrated that  
279 general inhibition of the mTOR pathway and specific inhibition of S6K1 lead to the further  
280 increase in Tau aggregation under long-term mitochondrial stress. In contrast, overactivation of  
281 the mTOR pathway, which caused increased phosphorylation of S6K1 and its substrate S6  
282 protein, significantly reduced Tau dimerization under long-lasting mitochondrial stress (Fig.  
283 4C). These results suggested that the increase in S6K1 phosphorylation that was present in the  
284 brains of Alzheimer's disease patients (An *et al.*, 2003) could be a beneficial adaptive response.  
285 Moreover, our observations showed that further activation of S6K1 could be a method for the  
286 reduction of Tau aggregation. In contrast, the reduction of increased phosphorylation of S6K1  
287 and S6 ribosomal protein, which was observed in mitochondrial myopathy, by mTOR inhibition  
288 caused the reversion of this mitochondrial disease (Khan *et al.*, 2017). It seems that for the  
289 reduction of mitochondrial myopathy progression, inhibition of S6K1 and S6 phosphorylation  
290 which leads to the reduction of protein synthesis was more beneficial. In the case of tauopathies  
291 more beneficial was maintaining the synthesis of essential proteins for neuron functioning and  
292 the production of proteins that maintain proteostasis like molecular chaperons. All these results  
293 demonstrated that the mTOR pathway is an important player in mitochondrial and  
294 neurodegenerative diseases but in order to obtain a therapeutic effect of pharmacological  
295 interventions, i.e. activation versus inhibition of the mTOR pathway, the treatment need to be  
296 tailored to the particular pathology.

297

298

299

300

301 **Acknowledgments**

302 We thank David Stroud and Michael Ryan for providing the HEK293T NDUFA11 knockout  
303 cell line, Malgorzata Urbańska and Jacek Jaworski for providing the HEK293T NDUFA11  
304 knockout cell line with shRNA-mediated knockdown of TSC2 and Minji Kim and Agnieszka  
305 Chacińska for valuable comments and discussions. This work was supported by National  
306 Science Centre of Poland (NCN), Grant Number 2019/33/B/NZ3/00533 (for LS).

307

308 **Author contributions**

309 LS conceived, designed, and supervised the study. LS and PO performed the experiments and  
310 analyzed the data. LS wrote the manuscript with the input of PO and MD.

311

312 **Conflict of interest**

313 The authors declare no conflict of interest.

314

315 **References**

316 An, W.L., Cowburn, R.F., Li, L., Braak, H., Alafuzoff, I., Iqbal, K., Iqbal, I.G., Winblad, B., and Pei,  
317 J.J. (2003). Up-regulation of phosphorylated/activated p70 S6 kinase and its relationship to  
318 neurofibrillary pathology in Alzheimer's disease. *Am J Pathol* 163, 591-607.

319 Blum, D., Herrera, F., Francelle, L., Mendes, T., Basquin, M., Obriot, H., Demeyer, D., Sergeant, N.,  
320 Gerhardt, E., Brouillet, E., Buee, L., and Outeiro, T.F. (2015). Mutant huntingtin alters Tau  
321 phosphorylation and subcellular distribution. *Hum Mol Genet* 24, 76-85.

322 Cabral-Costa, J.V., and Kowaltowski, A.J. (2020). Neurological disorders and mitochondria. *Mol*  
323 *Aspects Med* 71, 100826.

324 Hoover, B.R., Reed, M.N., Su, J., Penrod, R.D., Kotilinek, L.A., Grant, M.K., Pitstick, R., Carlson,  
325 G.A., Lanier, L.M., Yuan, L.L., Ashe, K.H., and Liao, D. (2010). Tau mislocalization to dendritic spines  
326 mediates synaptic dysfunction independently of neurodegeneration. *Neuron* 68, 1067-1081.

327 Khan, N.A., Nikkanen, J., Yatsuga, S., Jackson, C., Wang, L., Pradhan, S., Kivela, R., Pessia, A.,  
328 Velagapudi, V., and Suomalainen, A. (2017). mTORC1 Regulates Mitochondrial Integrated Stress  
329 Response and Mitochondrial Myopathy Progression. *Cell Metab* 26, 419-428 e415.

330 Lim, S., Haque, M.M., Kim, D., Kim, D.J., and Kim, Y.K. (2014). Cell-based Models To Investigate  
331 Tau Aggregation. *Comput Struct Biotechnol J* 12, 7-13.

- 332 Merkwirth, C., Martinelli, P., Korwitz, A., Morbin, M., Bronneke, H.S., Jordan, S.D., Rugarli, E.I., and  
333 Langer, T. (2012). Loss of prohibitin membrane scaffolds impairs mitochondrial architecture and leads  
334 to tau hyperphosphorylation and neurodegeneration. *PLoS Genet* 8, e1003021.
- 335 Nowicka, U., Chroscicki, P., Stroobants, K., Sladowska, M., Turek, M., Uszczynska-Ratajczak, B.,  
336 Kundra, R., Goral, T., Perni, M., Dobson, C.M., Vendruscolo, M., and Chacinska, A. (2021a). Cytosolic  
337 aggregation of mitochondrial proteins disrupts cellular homeostasis by stimulating the aggregation of  
338 other proteins. *eLife* 10, e65484.
- 339 Nowicka, U., Kim, M.J., and Chacinska, A. (2021b). Suppressing toxic aggregates: let MIA do it!  
340 *EMBO J* 40, e109001.
- 341 Samluk, L., Ostapczuk, P., and Dziembowska, M. (2022). Long-term mitochondrial stress induces early  
342 steps of Tau aggregation by increasing reactive oxygen species levels and affecting cellular proteostasis.  
343 *Mol Biol Cell* 33, ar67.
- 344 Samluk, L., Urbanska, M., Kisielewska, K., Mohanraj, K., Kim, M.J., Machnicka, K., Liszewska, E.,  
345 Jaworski, J., and Chacinska, A. (2019). Cytosolic translational responses differ under conditions of  
346 severe short-term and long-term mitochondrial stress. *Mol Biol Cell* 30, 1864-1877.
- 347 Schlagowski, A.M., Knoringer, K., Morlot, S., Sanchez Vicente, A., Flohr, T., Kramer, L., Boos, F.,  
348 Khalid, N., Ahmed, S., Schramm, J., Murschall, L.M., Haberkant, P., Stein, F., Riemer, J., Westermann,  
349 B., Braun, R.J., Winklhofer, K.F., Charvin, G., and Herrmann, J.M. (2021). Increased levels of  
350 mitochondrial import factor Mia40 prevent the aggregation of polyQ proteins in the cytosol. *EMBO J*  
351 40, e107913.
- 352 Sorrentino, V., Romani, M., Mouchiroud, L., Beck, J.S., Zhang, H., D'Amico, D., Moullan, N., Potenza,  
353 F., Schmid, A.W., Rietsch, S., Counts, S.E., and Auwerx, J. (2017). Enhancing mitochondrial  
354 proteostasis reduces amyloid-beta proteotoxicity. *Nature* 552, 187-193.
- 355 Stroud, D.A., Surgenor, E.E., Formosa, L.E., Reljic, B., Frazier, A.E., Dibley, M.G., Osellame, L.D.,  
356 Stait, T., Beilharz, T.H., Thorburn, D.R., Salim, A., and Ryan, M.T. (2016). Accessory subunits are  
357 integral for assembly and function of human mitochondrial complex I. *Nature* 538, 123-126.
- 358 Tak, H., Haque, M.M., Kim, M.J., Lee, J.H., Baik, J.H., Kim, Y., Kim, D.J., Grailhe, R., and Kim, Y.K.  
359 (2013). Bimolecular fluorescence complementation; lighting-up tau-tau interaction in living cells. *PLoS*  
360 *One* 8, e81682.
- 361 Topf, U., Suppanz, I., Samluk, L., Wrobel, L., Boser, A., Sakowska, P., Knapp, B., Pietrzyk, M.K.,  
362 Chacinska, A., and Warscheid, B. (2018). Quantitative proteomics identifies redox switches for global  
363 translation modulation by mitochondrially produced reactive oxygen species. *Nature communications*  
364 9, 324.
- 365 Tsuyama, T., Tsubouchi, A., Usui, T., Imamura, H., and Uemura, T. (2017). Mitochondrial dysfunction  
366 induces dendritic loss via eIF2alpha phosphorylation. *J Cell Biol* 216, 815-834.
- 367 Wang, X., Zuo, X., Kucejova, B., and Chen, X.J. (2008). Reduced cytosolic protein synthesis suppresses  
368 mitochondrial degeneration. *Nat Cell Biol* 10, 1090-1097.
- 369 Zheng, X., Boyer, L., Jin, M., Kim, Y., Fan, W., Bardy, C., Berggren, T., Evans, R.M., Gage, F.H., and  
370 Hunter, T. (2016). Alleviation of neuronal energy deficiency by mTOR inhibition as a treatment for  
371 mitochondria-related neurodegeneration. *eLife* 5, e13378.

372

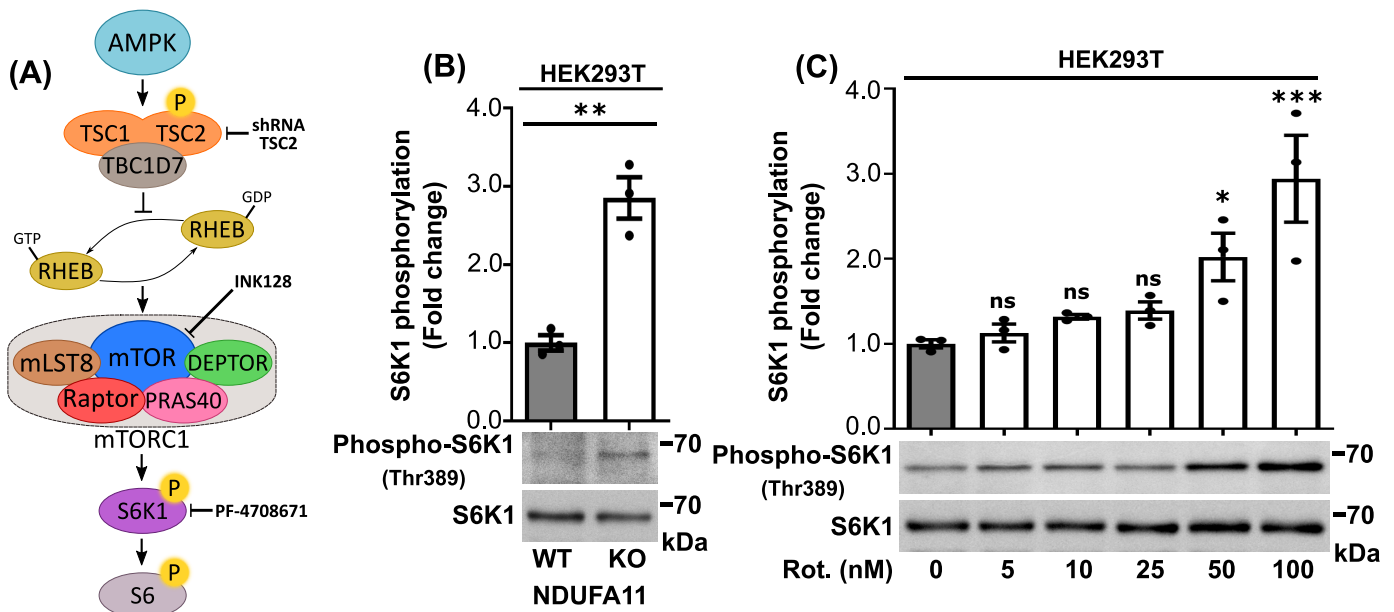


**Fig. 1.** Long-term mitochondrial stress increases S6K1 (Thr389) phosphorylation. (A) Schematic diagram of mTORC1 signaling. Stress-activated AMPK phosphorylates TSC2 protein (in complex with TSC1 and TBC1D7), which inhibits RHEB (mTORC1 activator), resulting in a reduction of mTORC1 activity. The main components of mTORC1 are mTOR kinase, Raptor, DEPTOR, PRAS40, and mLST8 proteins. The dephosphorylation of S6K1 causes inhibition of its substrate (S6 ribosomal protein), resulting in a reduction of protein synthesis at the ribosome. INK128 is an mTOR kinase inhibitor, PF-4708671 is an S6K1 inhibitor, shRNA TSC2 was used for silencing of TSC2 resulting in TSC1-TSC2-TBC1D7 complex inhibition. (B) Phosphorylation of S6K1 (Thr389) in HEK293T wild type cells and in HEK293T NDUFA11 deficient cells. The data are expressed as mean  $\pm$  SEM.  $n = 3$ . (C) Phosphorylation of S6K1 (Thr389) in HEK293T wild type cells that were treated for 48 h with rotenone. The data are expressed as mean  $\pm$  SEM.  $n = 3$ . Rot, rotenone. \* $p < 0.05$ ; \*\* $p < 0.01$ ; \*\*\* $p < 0.001$ ; ns, not significant ( $p > 0.05$ ) by Student's *t* test (1B) or one-way ANOVA followed by Dunnett's multiple comparisons test (1C).



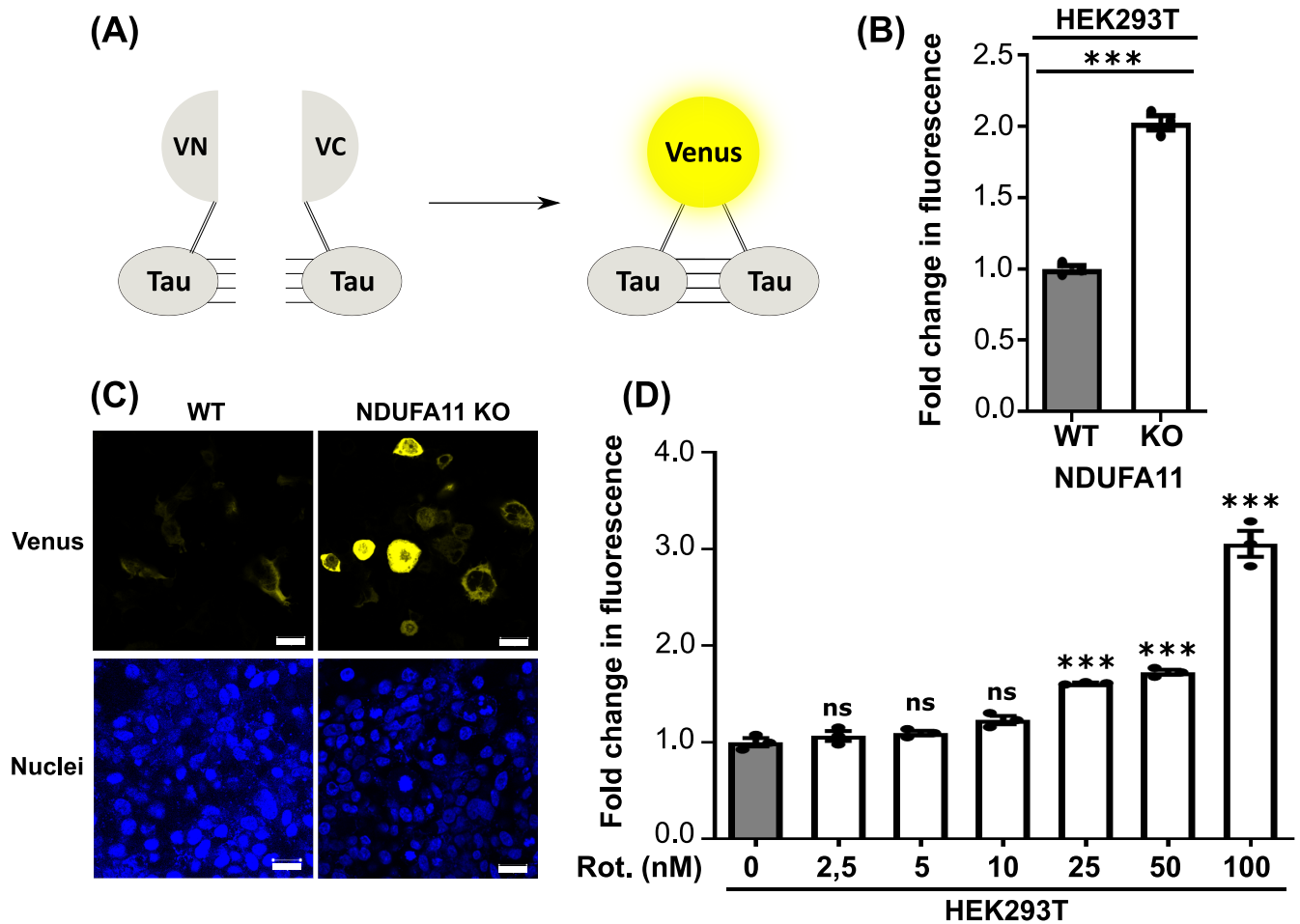


**Fig. 2.** Tau protein aggregates in HEK293T cells with mitochondrial respiratory chain complex I dysfunction. (A) The principle of the bimolecular fluorescence complementation (BiFC) assay. Cells were transfected with plasmids that encoded Tau protein that was fused with the N-terminal part of Venus protein (Tau-VN) and Tau protein that was fused with the C-terminal part of Venus protein (Tau-VC). Tau protein aggregation resulted in the reconstitution of Venus protein and the increase in fluorescence. (B) Flow cytometry analysis of Venus protein fluorescence in HEK293T wild type cells (WT) and in HEK293T NDUFA11 knockout cell line. The data are expressed as mean  $\pm$  SEM.  $n = 3$ . (C) Confocal images of Venus protein in HEK293T wild type (WT) cells and in HEK293T NDUFA11 deficient cells. Nuclei were stained with DAPI. Scale bar = 20  $\mu$ m. (D) Flow cytometry analysis of Venus protein fluorescence in HEK293T cells that were treated for 72 h with rotenone. The data are expressed as mean  $\pm$  SEM.  $n = 3$ . Rot, rotenone. \*\*\* $p < 0.001$ ; ns, not significant ( $p > 0.05$ ) by Student's t test (2B) or one-way ANOVA followed by Dunnett's multiple comparisons test (2D).



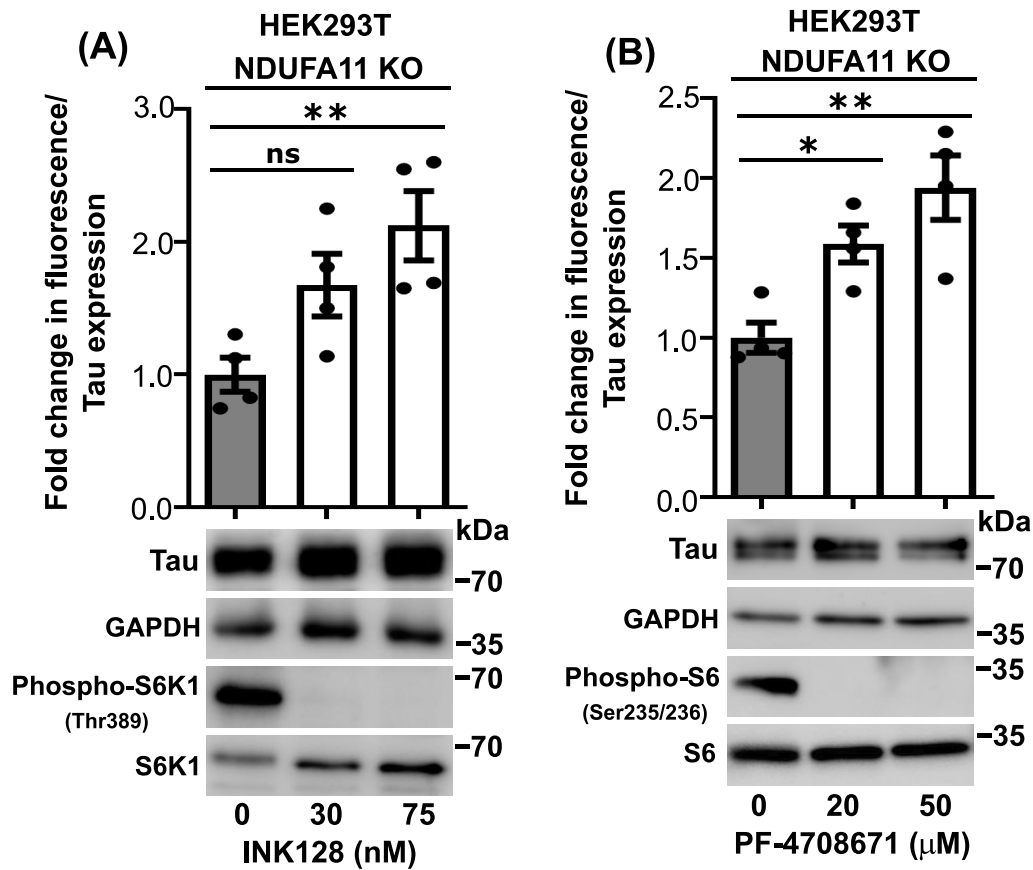


**Fig. 3.** The inhibition of mTOR or S6K1 protein increased Tau aggregation in HEK293T NDUFA11-deficient cells. (A) Fold change in Venus fluorescence normalized to the level of Tau expression in HEK293T NDUFA11 knockout cells that were treated for 3 h with INK128 as indicated. The data are expressed as mean  $\pm$  SEM.  $n = 4$ . (B) Fold change in Venus fluorescence normalized to the level of Tau expression in HEK293T NDUFA11 knockout cells that were treated for 24 h with PF-4708671 as indicated. The data are expressed as mean  $\pm$  SEM.  $n = 4$ . \* $p < 0.05$ ; \*\* $p < 0.01$ ; ns, not significant ( $p > 0.05$ ) (One-way ANOVA followed by Tukey's multiple comparisons test).

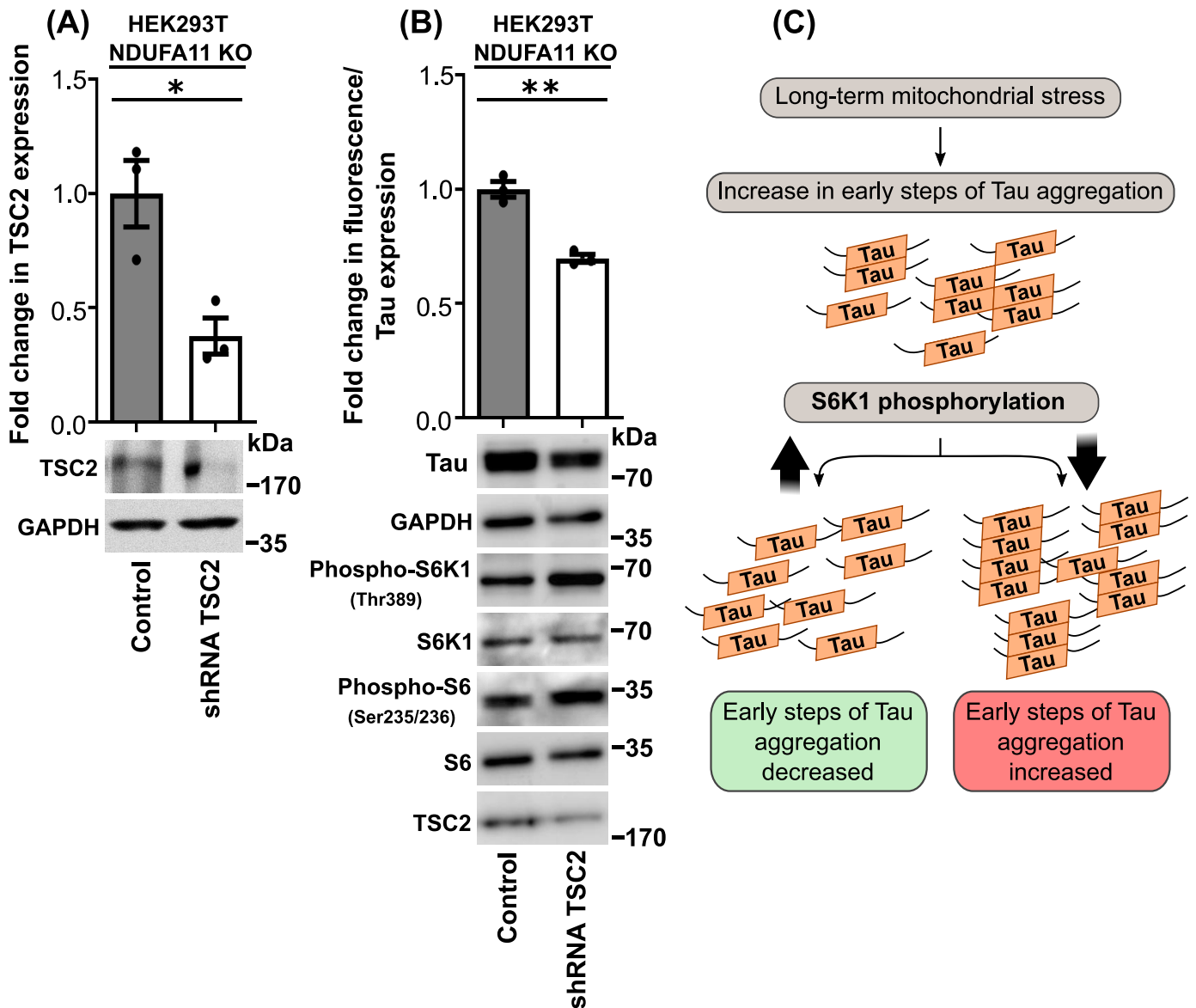


**Fig. 4.** The knockdown of TSC2 protein reduced Tau aggregation in HEK293T NDUFA11-deficient cells. (A) Fold change in TSC2 expression in HEK293T NDUFA11 knockout cells with stable shRNA-mediated knockdown of TSC2 protein. The data are expressed as mean  $\pm$  SEM.  $n = 3$ . (B) Fold change in Venus fluorescence normalized to the level of Tau expression in HEK293T NDUFA11 knockout cells with stable shRNA-mediated knockdown of TSC2 protein. The data are expressed as mean  $\pm$  SEM.  $n = 3$ . (C) Schematic illustration of the influence of S6K1 phosphorylation on Tau protein aggregation under long-term mitochondrial stress. \* $p < 0.05$ ; \*\* $p < 0.01$  (Student's  $t$  test).